



CENTRE NATIONAL
DE LA RECHERCHE
SCIENTIFIQUE



Dust charging and dust-surface interaction in the laboratory

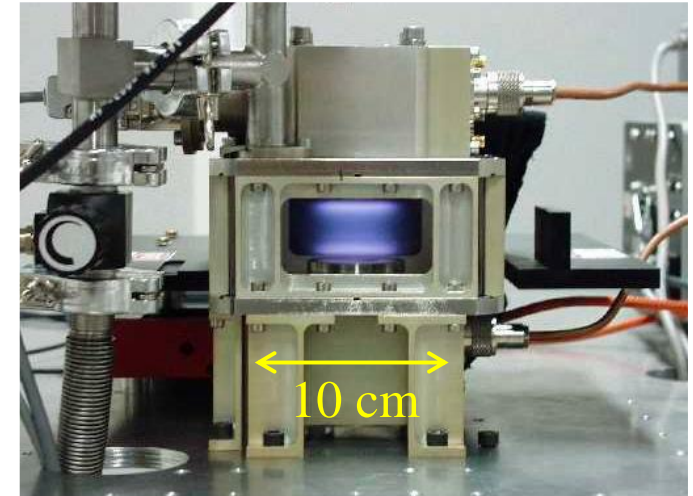
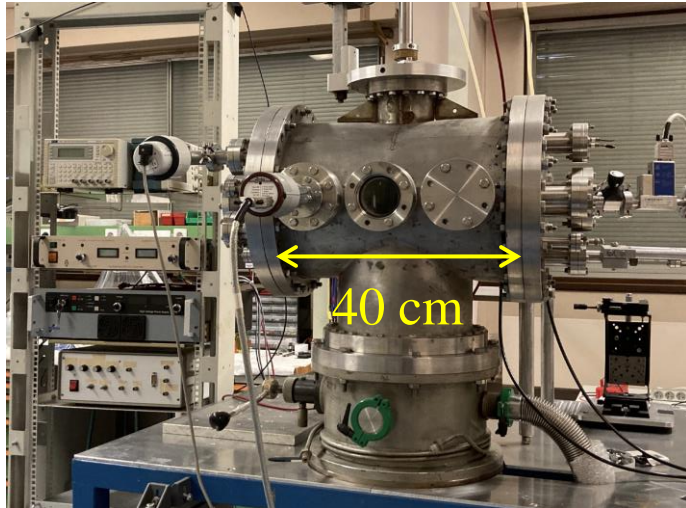
Cécile Arnas

Laboratory of Physics of Ions-Molecules Interaction (PIIM)

CNRS, Aix-Marseille university, 13013 Marseille, France

Workshop on Dust Charging and Beam-Dust Interaction in Particle Accelerators, CERN (13-15 June 2023)

Discharge chambers for dust-nanoparticle production

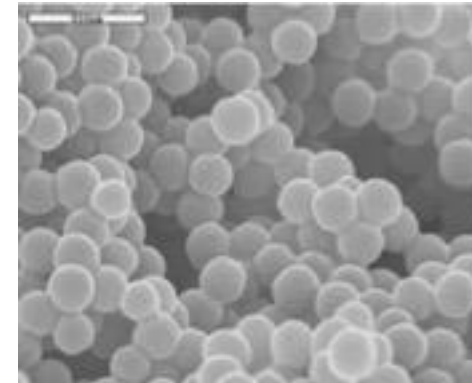
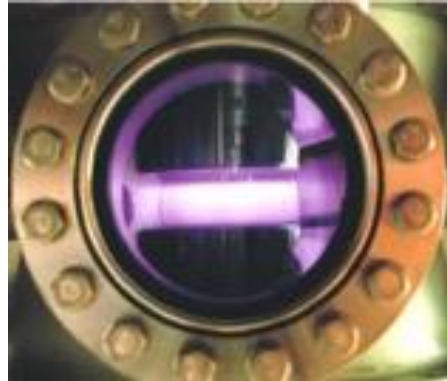


Base vacuum: from 10^{-5} Pa to 10^{-4} Pa

Plasmas (gas): 10 - 100 Pa

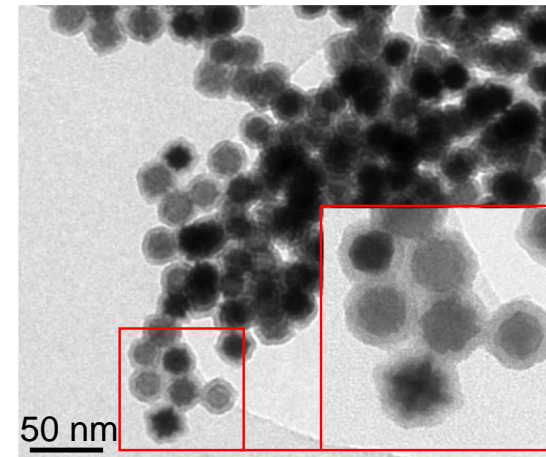
Discharges between electrodes in reactive gases

98% Ar plasmas mixed with 2% methane



carbonaceous
nanoparticles
 ≈ 200 nm

Ar plasma with sputtered atoms



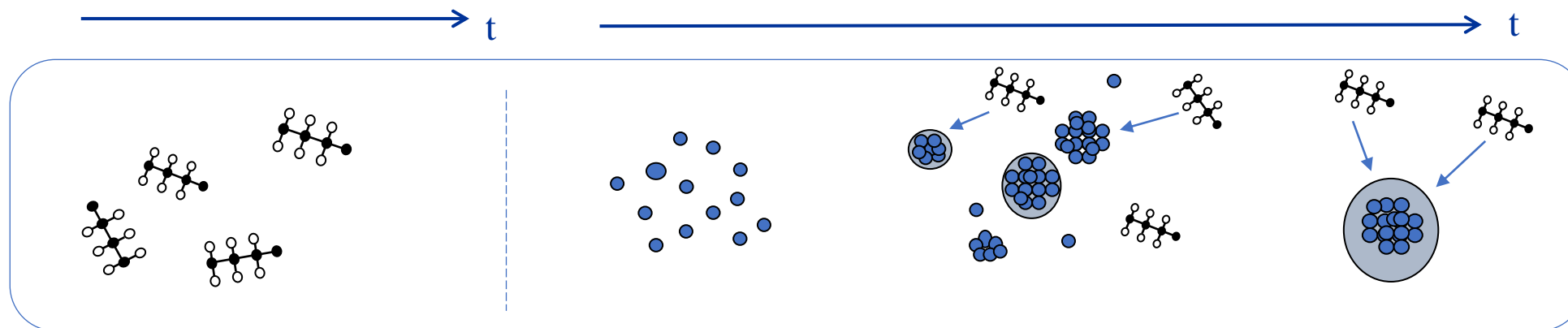
W nanoparticles
 ≈ 25 nm

Nanoparticles produced from cathode sputtering in DC discharges

- Size evolution, density, internal structure (indication on growth mechanisms)
- Modification of the discharge parameters during negative charging
- Modeling of charging mechanisms
- Transport inside the plasma

Molecular (ion, neutral) precursors

Nanoparticles

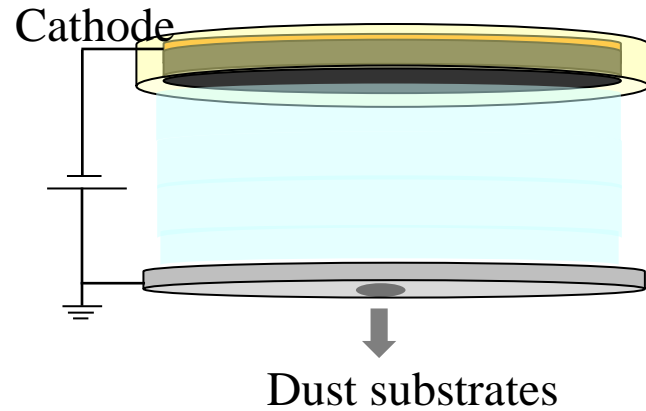


Specific collisions/reactions
(complex plasma chemistry)

Nucleation
(nuclei of 1-4 nm)

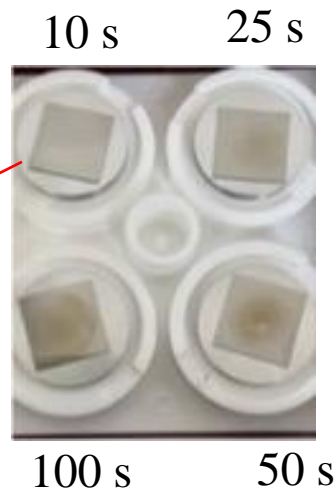
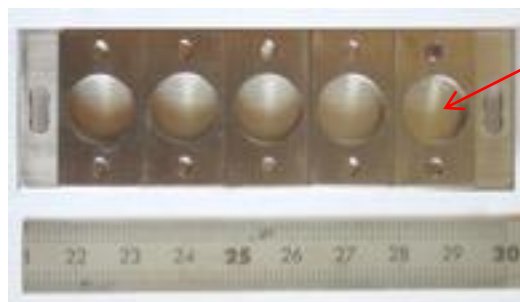
Agglomeration

Molecular sticking



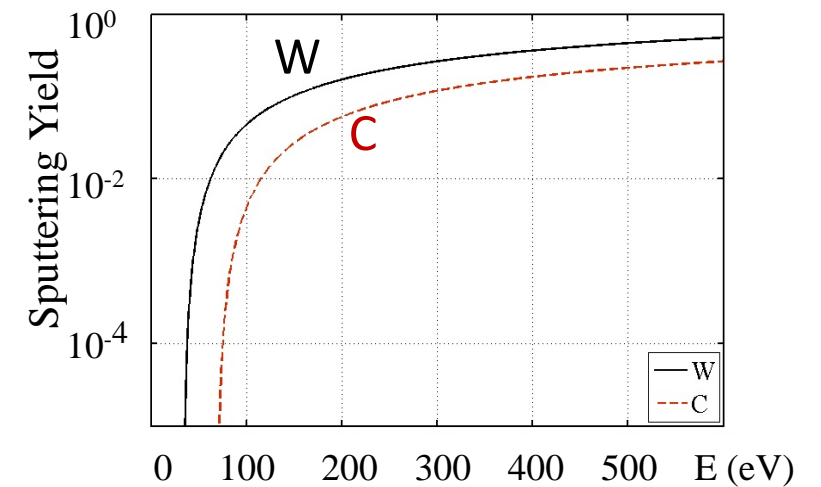
- Ar (30-60 Pa)
- Ar⁺ accelerated in the cathode sheath

Substrate holder

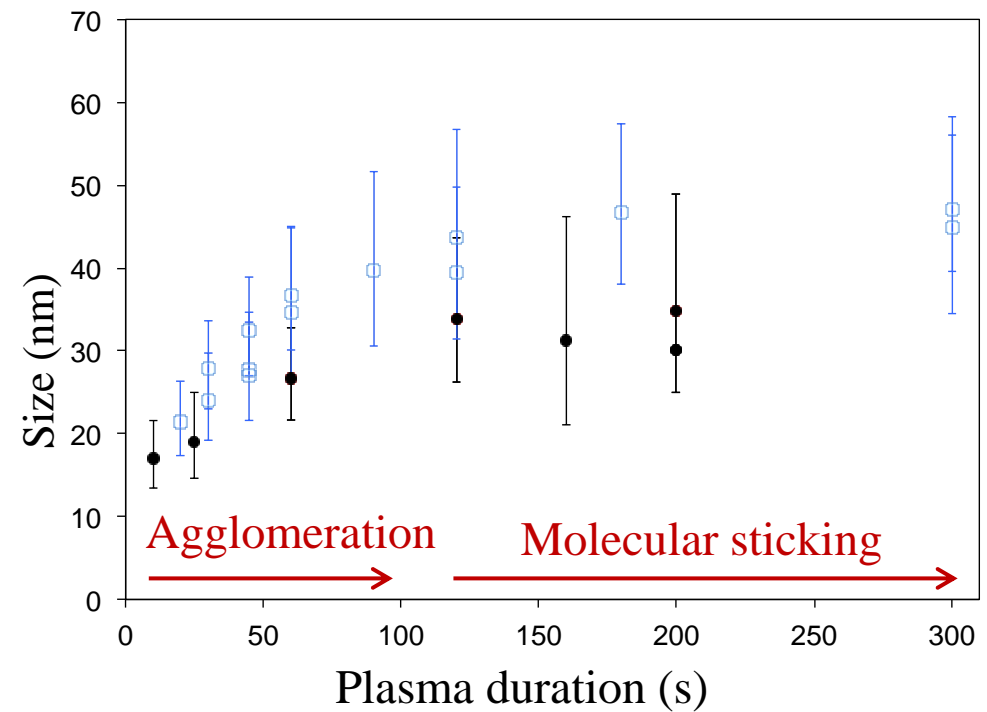


Cathode sputtering with energetic Ar⁺

- sputtering threshold (Ar/C) ~ 70 eV
- sputtering threshold (Ar/W) ~ 34 eV

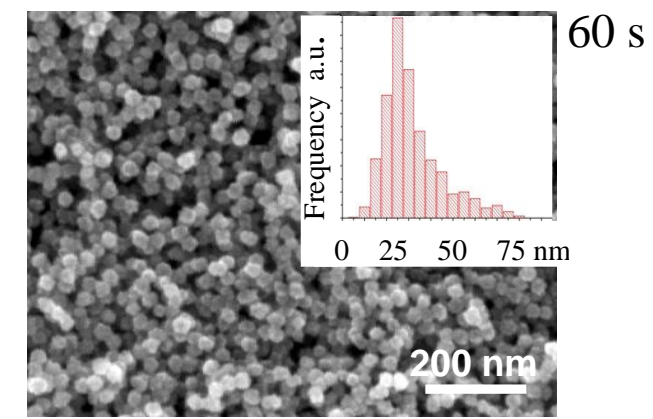
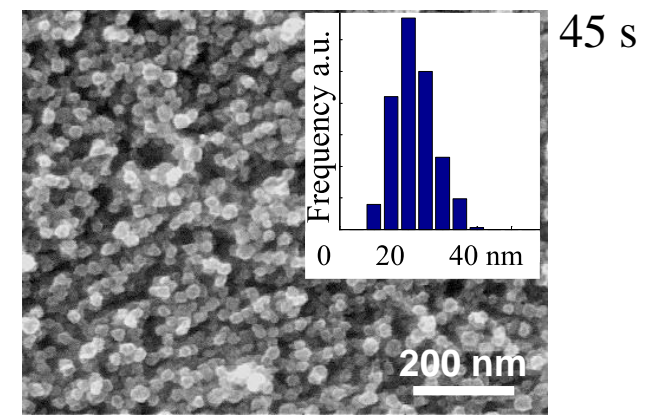


Size increase vs plasma duration



Flux of sputtered atoms:
 $\Gamma_C \sim \Gamma_W \sim 10^{18} \text{ m}^{-2}\text{s}^{-1}$

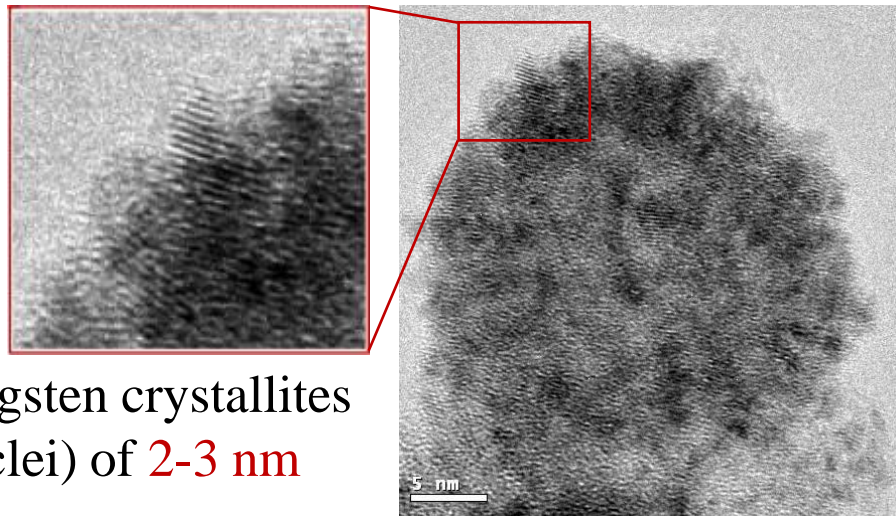
— Carbon nanoparticles
 — Tungsten nanoparticles



SEM images

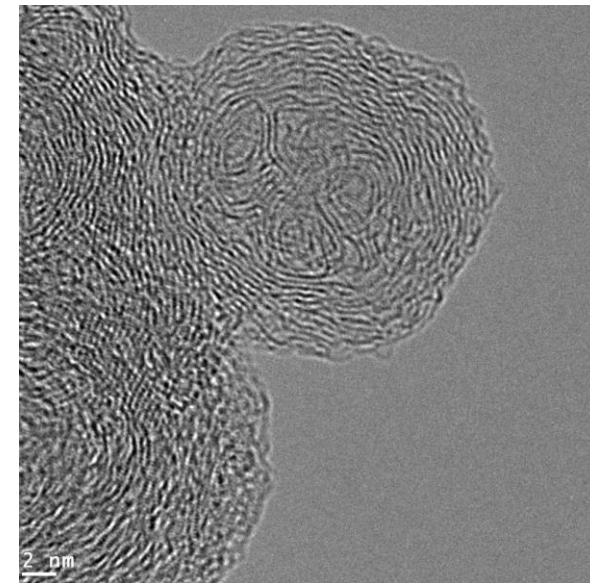
TEM-HR image

60 s



Tungsten crystallites
(nuclei) of **2-3 nm**

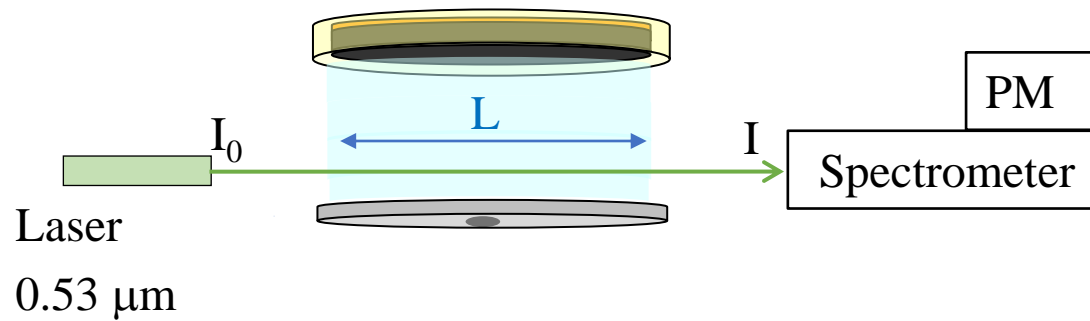
Tungsten nanoparticle **~ 28 nm**



Carbon nanoparticle **~ 25 nm**

Nuclei of **~ 3 nm**

Carbon sticking around



Beer-Lambert law: $I/I_0 = \exp(-\pi a^2 C_{\text{ext}} n_d L)$

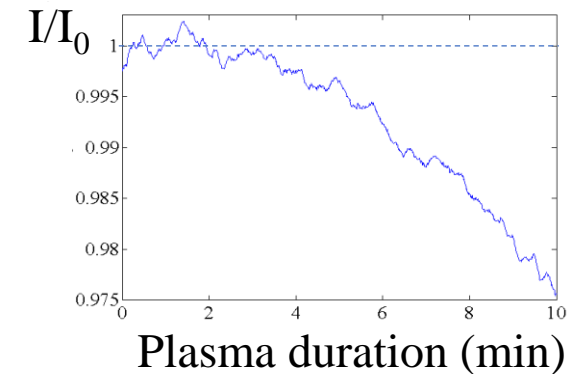
Extinction coefficient: $C_{\text{ext}} = C_{\text{abs}} + C_{\text{scat}}$ and $x = 2\pi a/\lambda_0 < 0.3$

$$C_{\text{abs}} = 4\pi \text{Im} \left[\frac{m^2 - 1}{m^2 + 2} \right], \quad C_{\text{scat}} = \frac{8}{3} x^4 \left| \frac{m^2 - 1}{m^2 + 2} \right|^2$$

m = complex refractive index of **carbon nanoparticle**

$$m = 1.3 + i 0.08$$

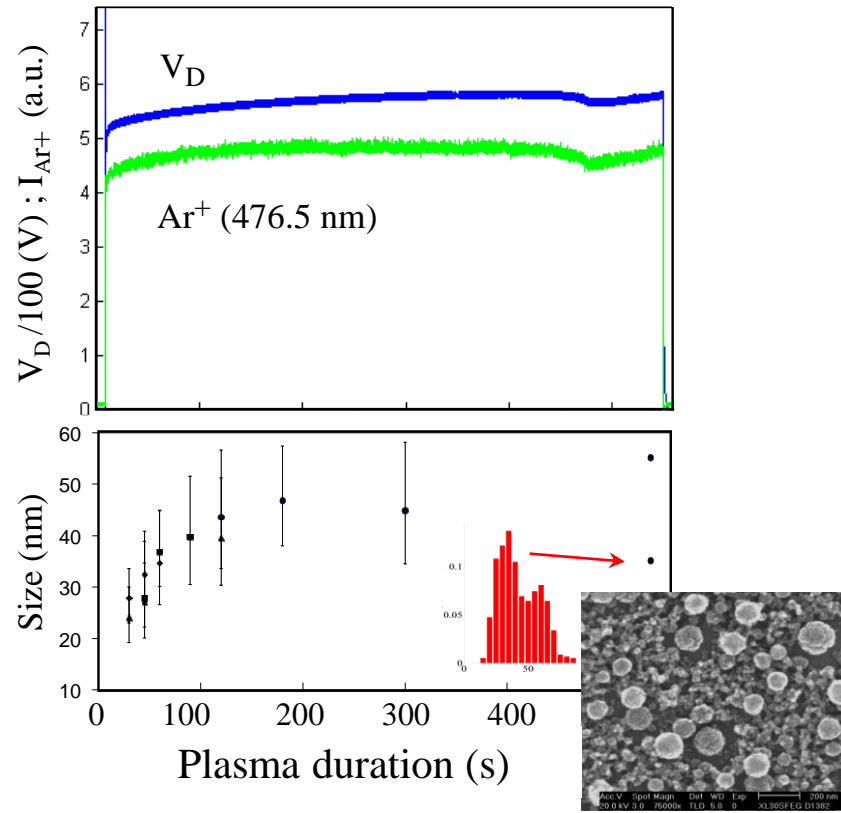
Carbon nanoparticles:



$2a \sim 55 \text{ nm}$
 $t = 600 \text{ s}$

$$n_{\text{NP}} \sim 2 \cdot 10^8 \text{ cm}^{-3}$$

Charging of carbon nanoparticles to the detriment of discharge/plasma



Three discharges parameters : $P_{Ar} = 60$ Pa, $I_d = 70$ mA,

V_d : self-regulated parameter (control the ionization)

No sputtering: P_{Ar} , I_d , V_d are cte

With sputtering and NPs production:

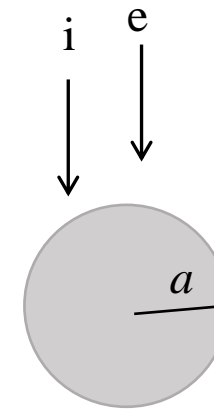
- Compensation of the electron loss by the increase of V_d
- decrease of V_d due to the loss of a part of NPs on the anode
- Increase again due to the appearance of a new NP generation

Maxwellian e^- and ions: $T_e < 5 \text{ eV}$ and $T_e \gg T_i \sim T_g$

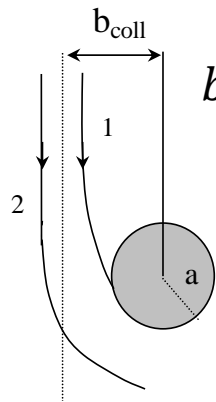
Dust charge (vacuum approximation): $Q = C\varphi \approx 4\pi\epsilon_0 a\varphi = Ze$

Looking for φ , the floating potential : $J_i(\varphi) - J_e(\varphi) = 0$

higher mobility of e^- : $\varphi < 0$



Orbital Motion Limited model (OML):



$$b_{coll}^2 = a^2 \left(1 - \frac{e\varphi}{k_B T_i}\right)$$

Ion current : $I_i = \frac{1}{4} \pi a^2 e n_0 v_i \left(1 - \frac{e\varphi}{k_B T_i}\right)$

$$\exp\left(\frac{e\varphi}{k_B T_e}\right) = \left(\frac{T_i m_e}{T_e m_i}\right)^{\frac{1}{2}} \left(1 - \frac{e\varphi}{k_B T_i}\right)$$

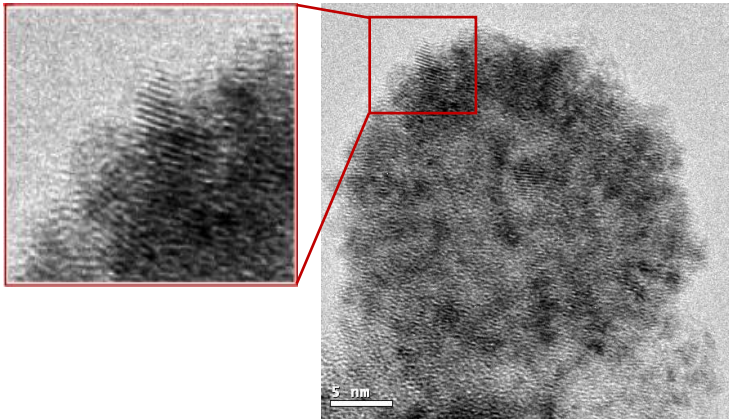
From Boltzman law:

Electron current : $I_e = -\frac{1}{4} \pi a^2 e n_0 v_e \exp\left(\frac{e\varphi}{k_B T_e}\right)$

For $T_e = 2 \text{ eV}$, $T_i = 0.04 \text{ eV}$

OML $\rightarrow \varphi = -4.3 \text{ eV}$

$a \sim 2\text{-}3 \text{ nm}$: $Z \sim 6e^- - 9e^-$



$a = 14 \text{ nm}$: $Z \sim 42 e^-$

- OML cannot explain agglomeration (Coulomb repulsion)
- Consider **charge fluctuations** \rightarrow nuclei can be briefly neutrals, positively charged

Charge distribution (T. Matsoukas *et al*, J. Appl. Phys.,1995)

- n_q : fraction of nanoparticles carrying the charge q

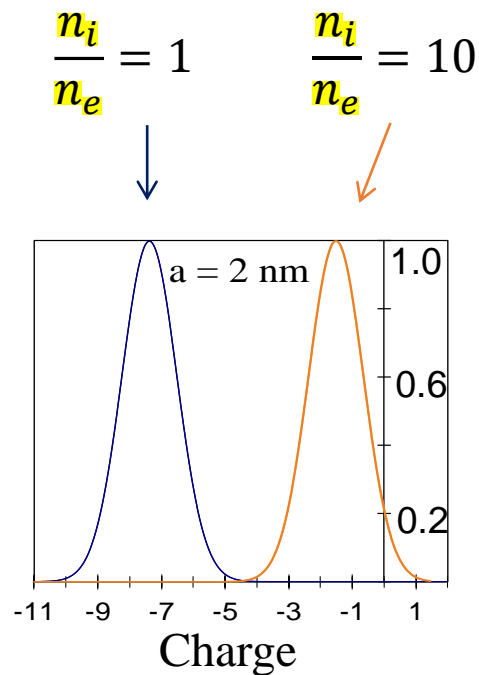
$$\frac{\partial n_q}{\partial t} = I_i(q-1)n_{q-1} + I_e(q+1)n_{q+1} - [I_e(q) + I_i(q)]n_q$$

- Transformed to a partial differential equation:

$$\frac{\partial n}{\partial t} = - \frac{\partial (I_i - I_e)n}{\partial q} + \frac{1}{2} \frac{\partial^2 (I_i + I_e)n}{\partial q^2}$$

Gaussian charge distribution:
$$n(q) = \frac{1}{\sigma\sqrt{2\pi}} \exp\left(-\frac{(q-\bar{q})^2}{2\sigma^2}\right)$$

Average charge:
$$\bar{q} = k \frac{4\pi\epsilon_0 a T_e}{e^2} \ln \left[\frac{n_i}{n_e} \left(\frac{m_e T_e}{m_i T_i} \right)^{1/2} \right]$$



- $\bar{q} \sim 7e$ when $n_i / n_e = 1$
- $\bar{q} \sim 2e$ when $n_i / n_e = 10$

Explains the nanoparticle growth by agglomeration
of nuclei at the condition of n_e depletion

→ charging to the detriment of plasma electrons

3 coupled numerical modules*: argon DC discharge – molecular ions formation – NP evolution

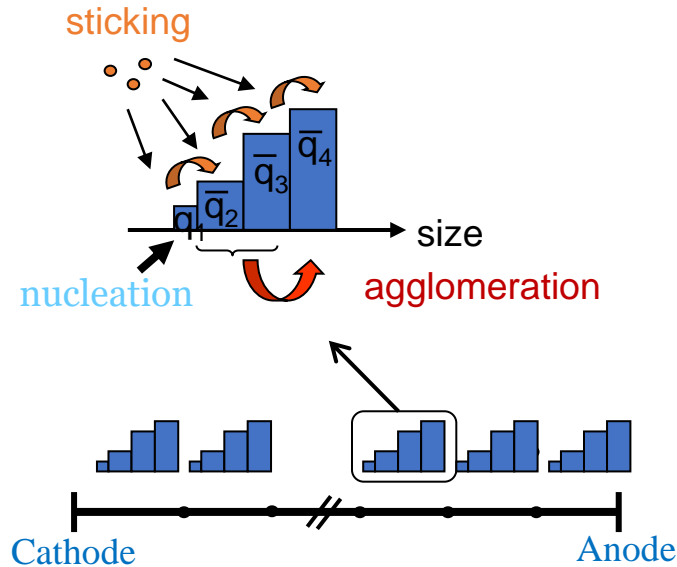
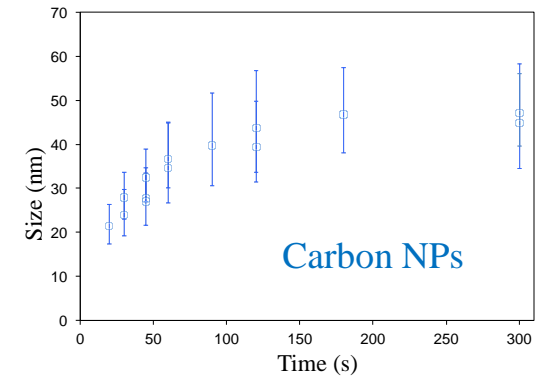
1D sectional model: size distribution divided into bins or sections along the plasma

In each section: sizes 1-100 nm

100 continuity eq for the total volume density

+ 100 eq for the average charge

- Nucleation
- Transport
- Growth by sticking
- Growth by agglomeration



NP volume balance in each section

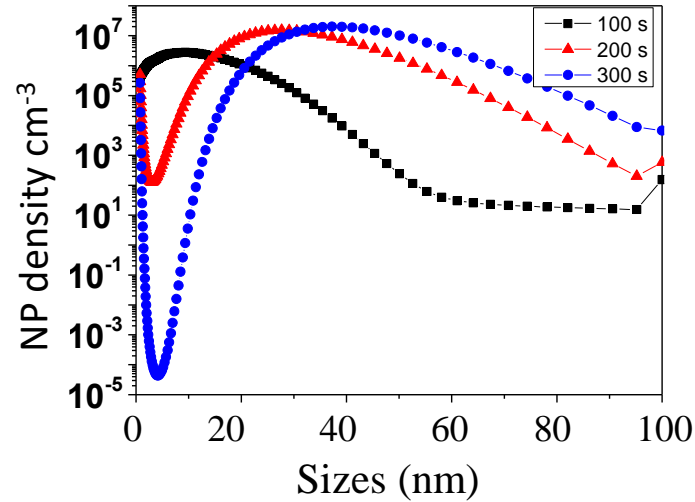
$$\frac{\partial V_l}{\partial t} = \frac{\partial V_l}{\partial t}_{aggl} + \frac{\partial V_l}{\partial t}_{stick} + S_{nuc} - \nabla F_l$$

Averaged NP charge of each section:

$$\frac{\partial q_l}{\partial t} = -\frac{\vec{\nabla}(q_l \vec{F}_l)}{V_l} + (I_{e-slow} + I_{e-fast} + I_i) S_l + S^q_{nuc} + S^q_{aggl} + S^q_{sticking}$$

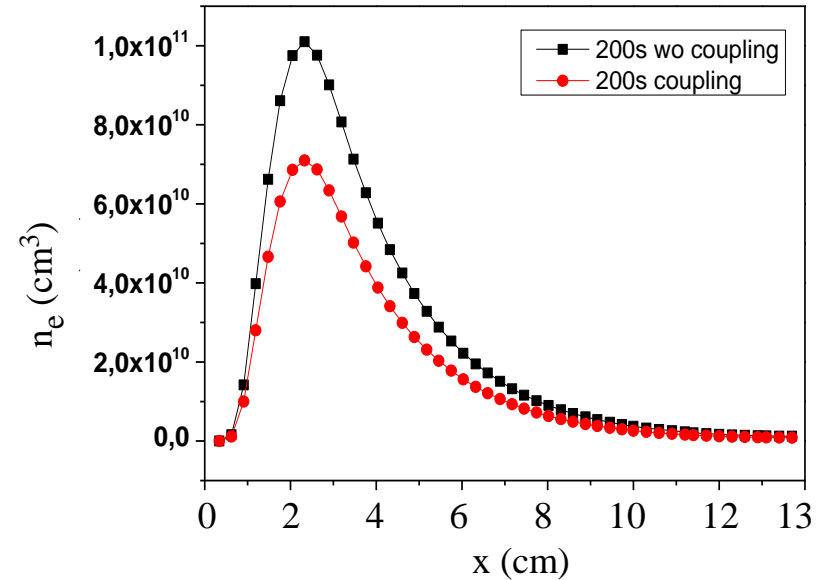
Gaussian charge distribution: smallest NPs can be neutral or > 0

*A. Michau, K. Hassouni et al, *Plasma Chem. Plasma Process.* **32** (2012); *J. Appl. Phys.* **121** (2017)



At $x \sim 2$ cm from the cathode
(position of electric field reversal)

Agglomeration can only occur between
nuclei (neutral, positively charged)
and big nanoparticles (negatively charged)



Red curve:

n_e calculated self-consistently through
the coupling of the 3 numerical modules:
coupling of negative molecular ions,
negatively charged nanoparticles and n_e

Nanoparticles produced from cathode sputtering in DC discharges

- ❑ Size evolution, internal structure (indications on formation), density
- ❑ Modification of the discharge parameters at large density
- ❑ Modeling of charging mechanisms (agglomeration)
- ⇒ ❑ Transport inside the plasma

- *Electric force* : $F_e = ZeE$ ($E = -\nabla V_p$ where V_p : plasma potential)

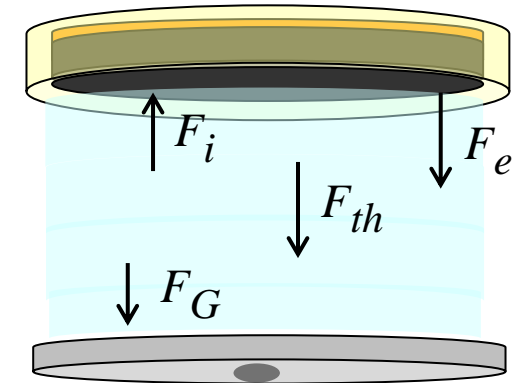
- *Ion drag force* : $F_i = 2/3\pi a^2 n_0 m_{ar} v_i u_i (1 - \frac{\rho_0}{2a} + \frac{\rho_0^2}{4a^2} \Lambda)$

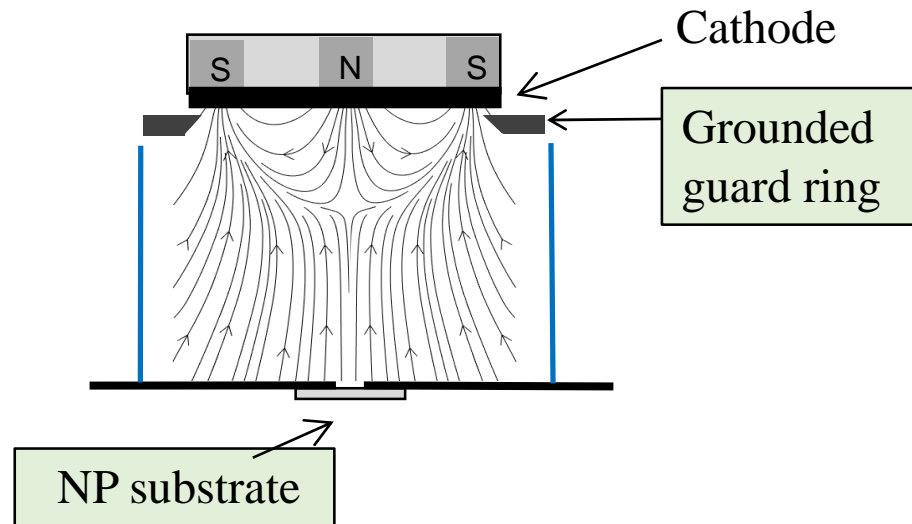
$$\rho_0 = \frac{Ze^2}{m_i v_{th}^2} : \text{Coulomb radius}$$

Λ : Coulomb logarithm

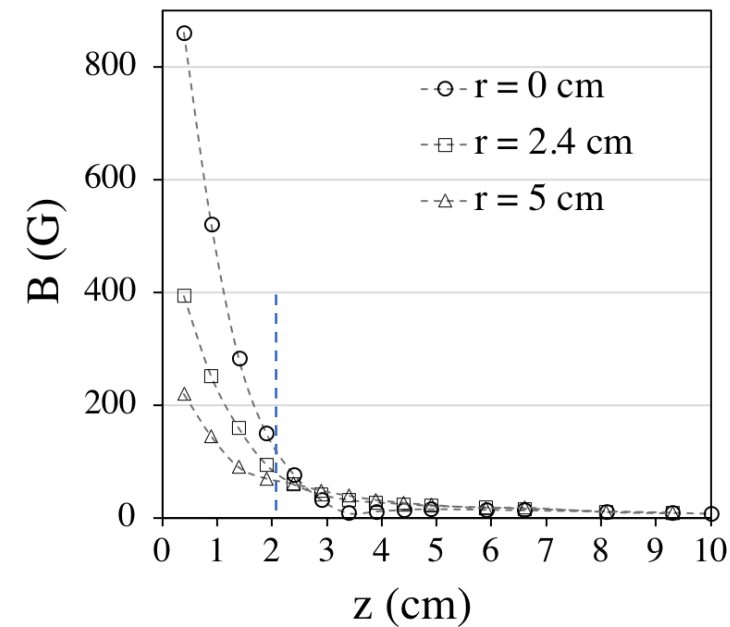
- *Thermophoretic force* : $F_{th} = -\frac{32}{15} \frac{a^2}{v_{th}} k_{th} \nabla T_{ar}$

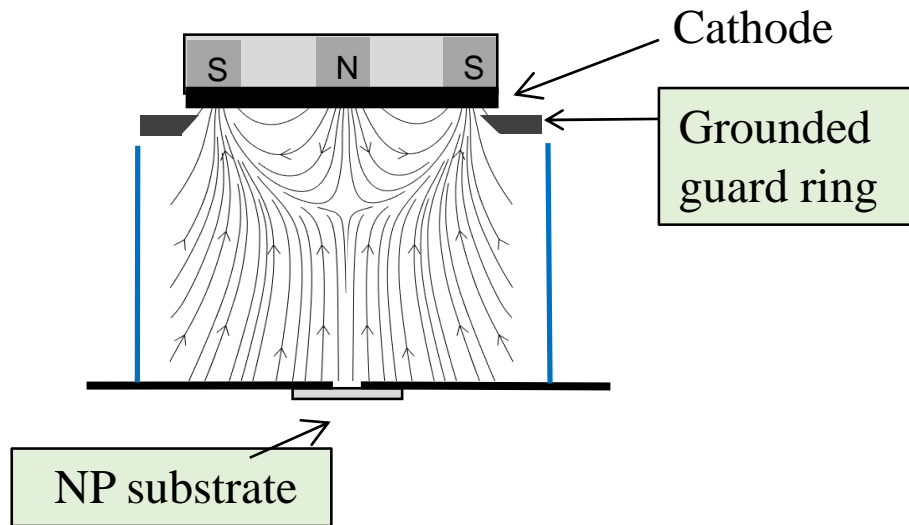
- *Gravity*: $F_G = 4/3\pi a^3 \rho g$ (negligible)





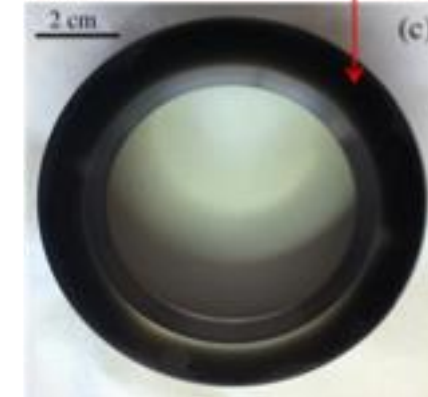
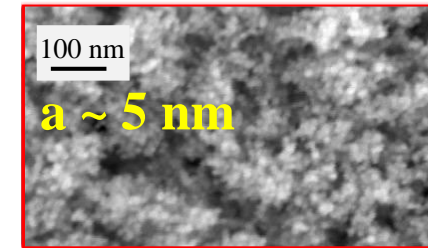
- Tungstène cathode (sputtering)
- $P_{ar} = 30 \text{ Pa}$, $I_d = 0.3 \text{ A}$ ($V_d \sim 200 \text{ V}$)



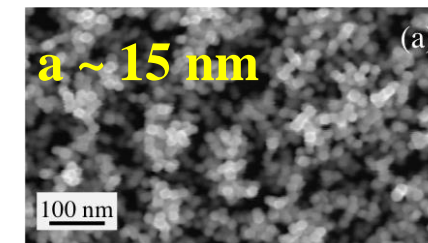


- Tungstène cathode (sputtering)
- $P_{ar} = 30 \text{ Pa}$, $I_d = 0.3 \text{ A}$ ($V_d \sim 200 \text{ V}$)

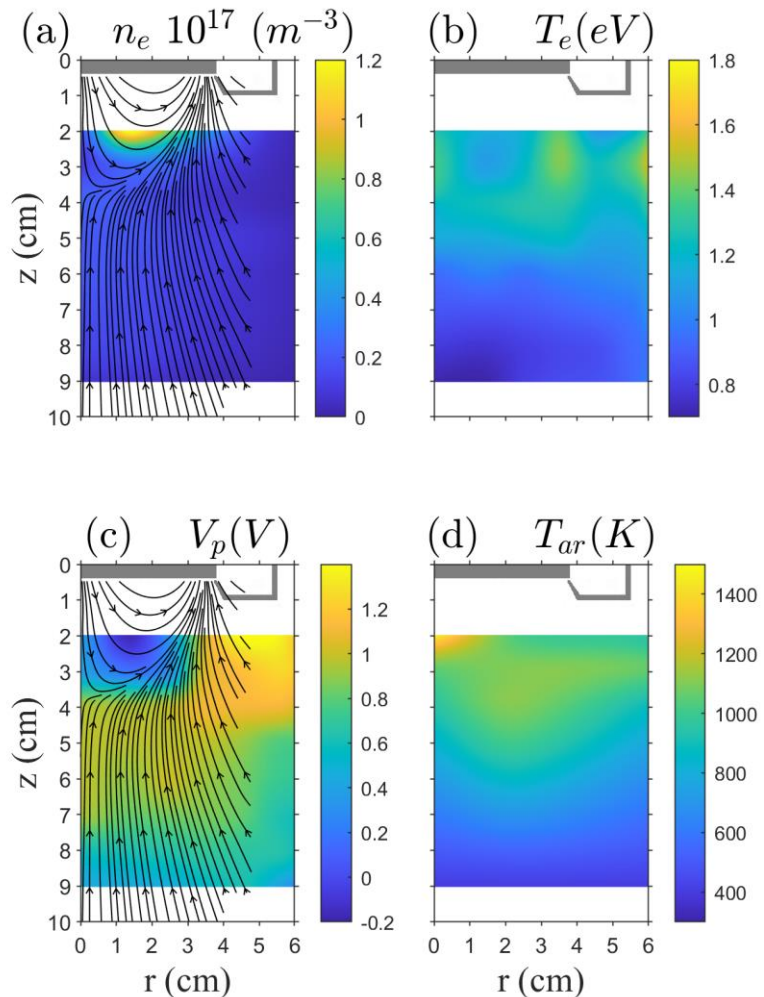
(10 successive plasmas of 200s)



Guard ring



NP substrate

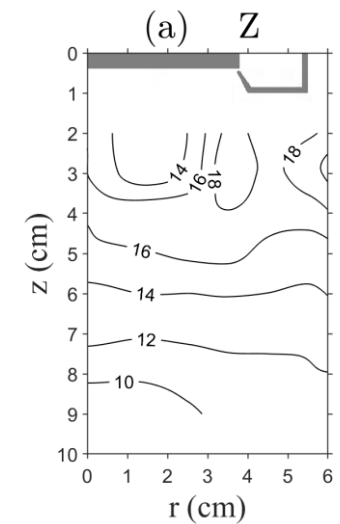


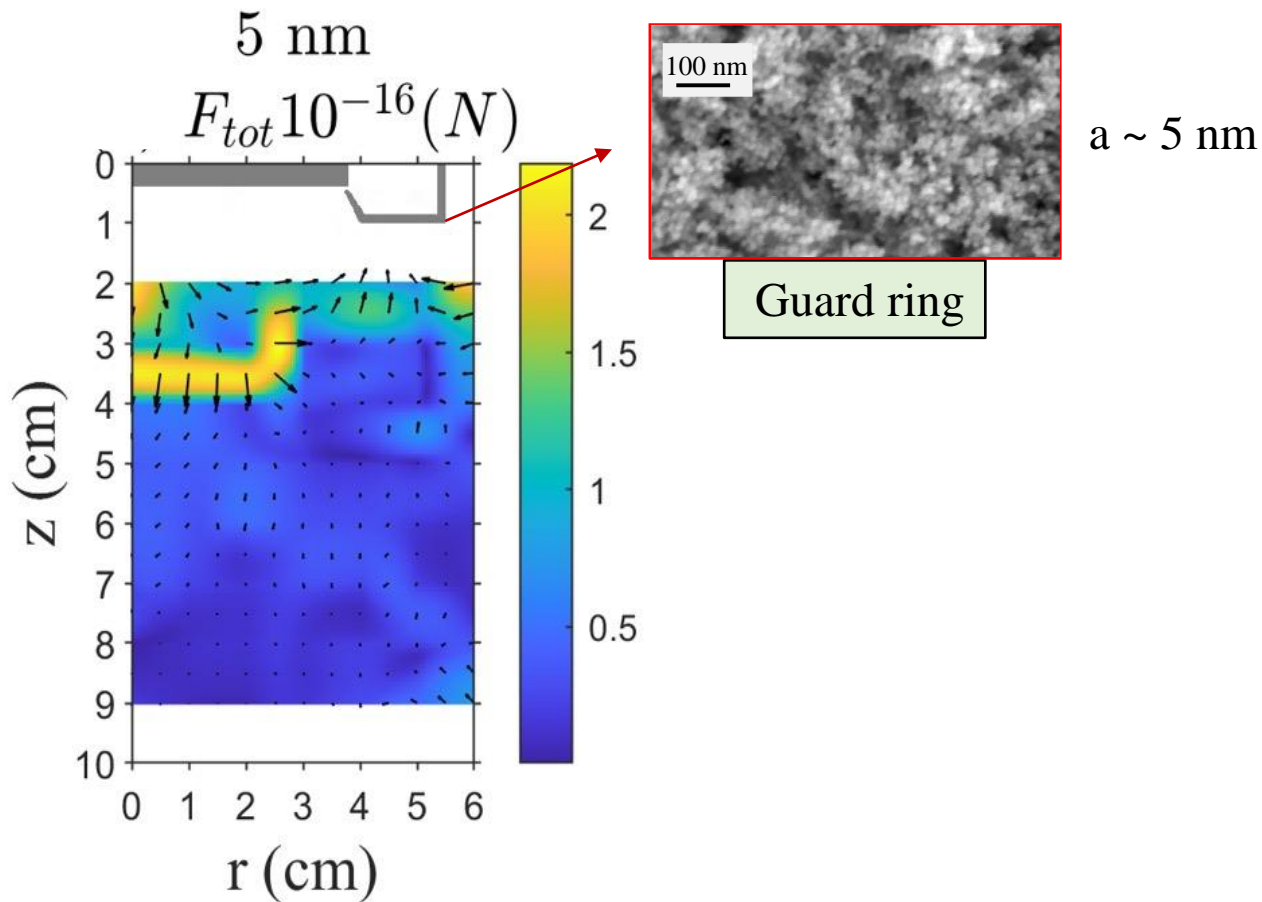
n_e , T_e , V_P : Langmuir probe measurements

T_{ar} : measurement by LIF

- n_e : maximum inside magnetic arches
- T_e : inverse variation of n_e
- V_P : increase inside magnetic arches
max after the last magnetic arch
- T_{ar} : Ar heating due to collisions
with sputtered atoms of $\langle E \rangle \sim 12$ eV

OML model; $a = 5$ nm





$$F_e + F_{th} + F_i = 0$$

negligible

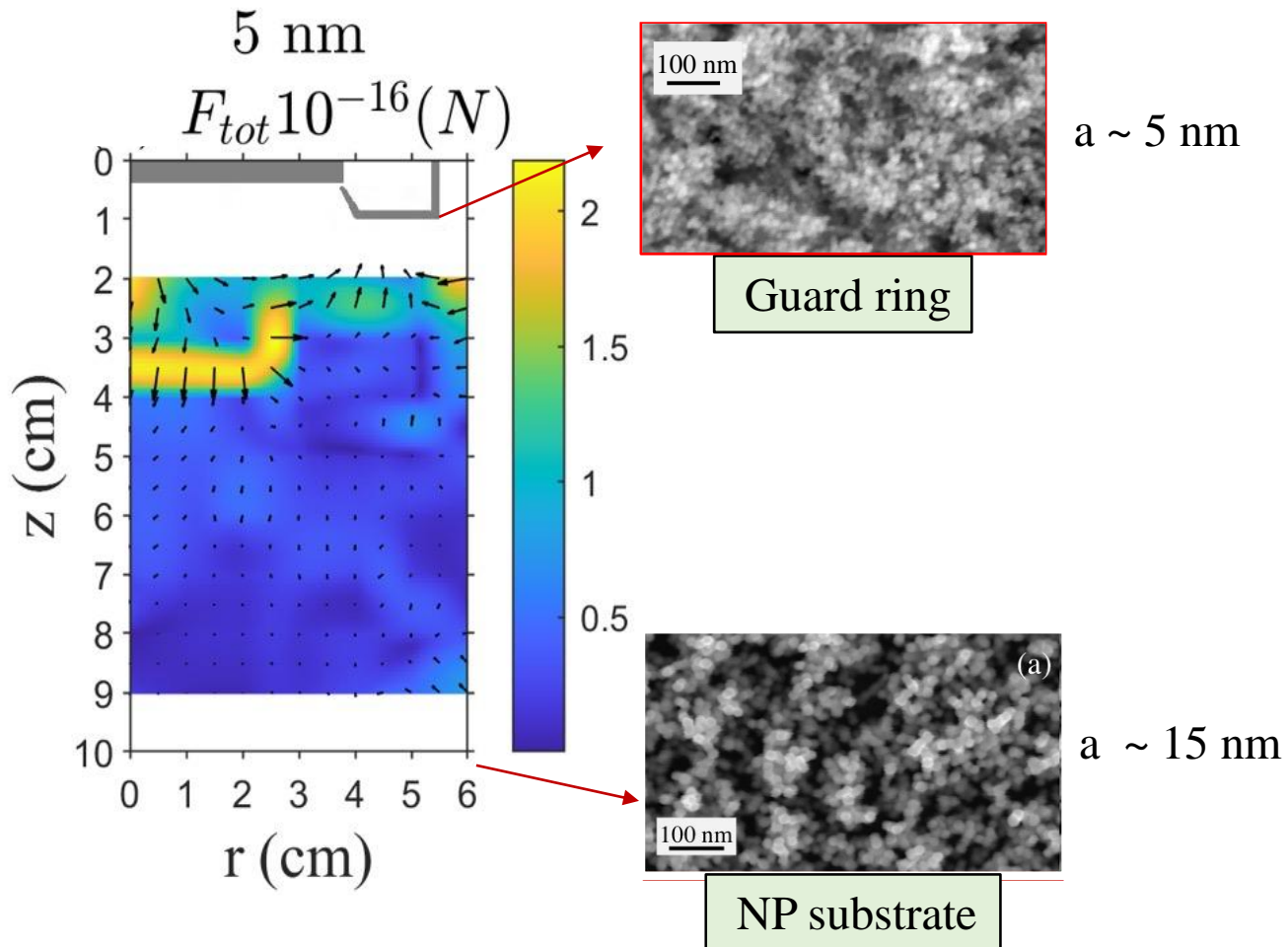
Upper part:

F_e and F_{th} : same range of values

- nanoparticles under the guard ring are pushed to the the guard ring
- near the axis: pushed outside magnetic arches and downwards

Lower part:

- F_{th} is dominant: pushed down



$$F_e + F_{th} + F_i = 0$$

negligible

Upper part:

F_e and F_{th} : same range of values

- nanoparticles under the guard ring are pushed to the the guard ring
- near the axis: pushed outside magnetic arches and downwards

Lower part:

- F_{th} is dominant: pushed down

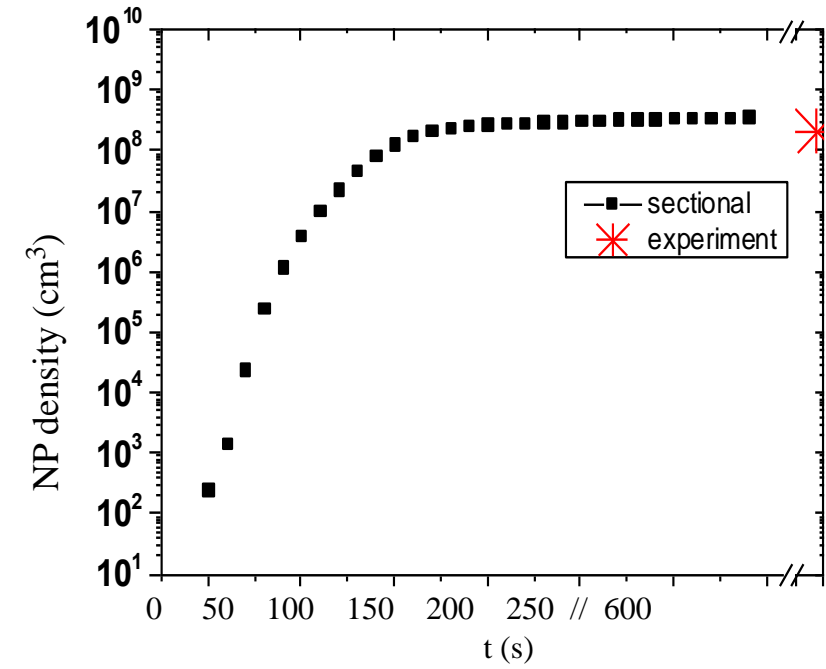
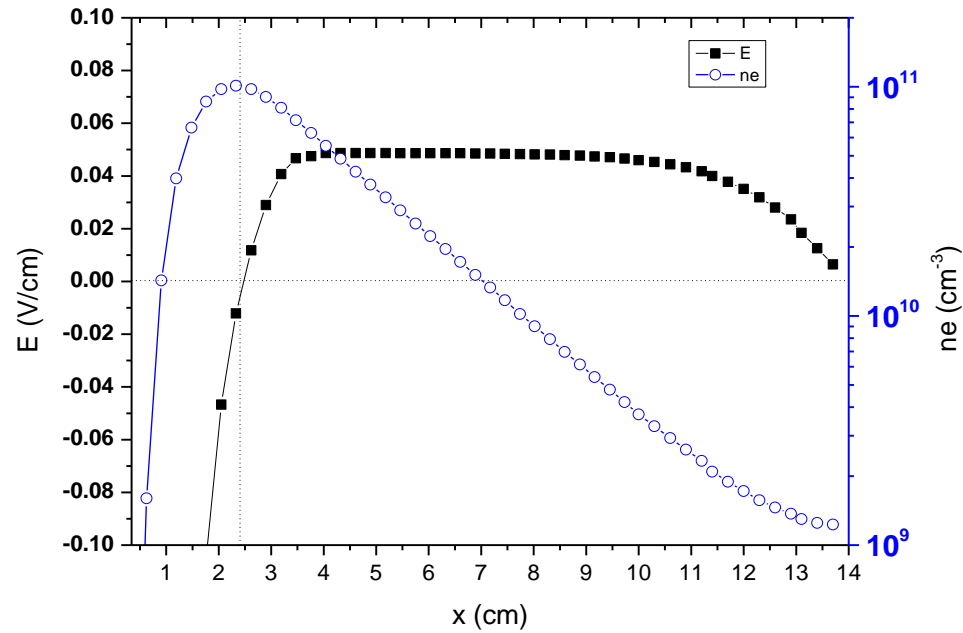


When NPs are transported down they have more “space, time” to grow than NPs near the guard ring

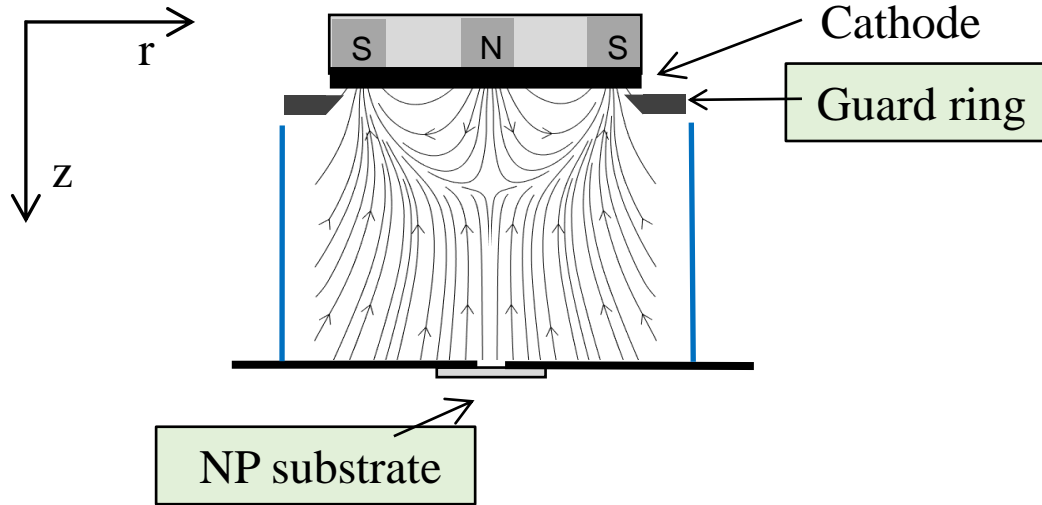
Nanoparticles produced from cathode sputtering in DC discharges

- ❑ Size evolution, density, internal structure (growth by agglomeration, sticking)
- ❑ Modification of the discharge parameters due to their negative charge
- ❑ Various modeling of charging mechanisms (+ fluctuations) and growth
- ❑ Applied forces for their transport in the plasma

Additional slides



NP density reaches $\sim 10^8$ cm⁻³
also found experimentally



- Cylindrical Langmuir probe

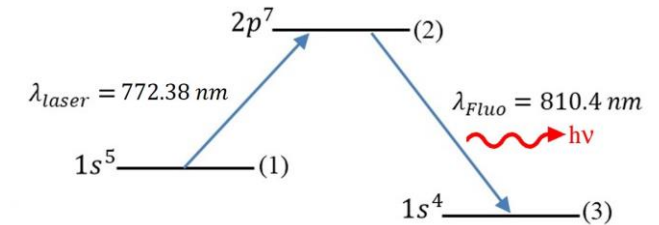
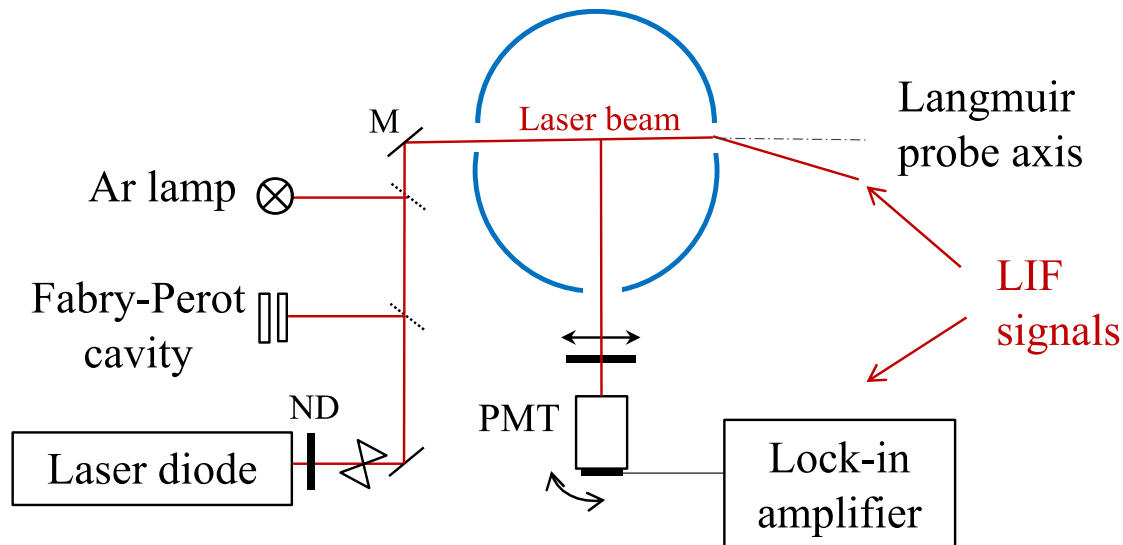
$r_{LP} \ll r_{larmor}$ for $z > 2$ cm and probe \perp B

(also) $v_{de}/v_{the} \leq 0.32$



Classical analyses of probe characteristics

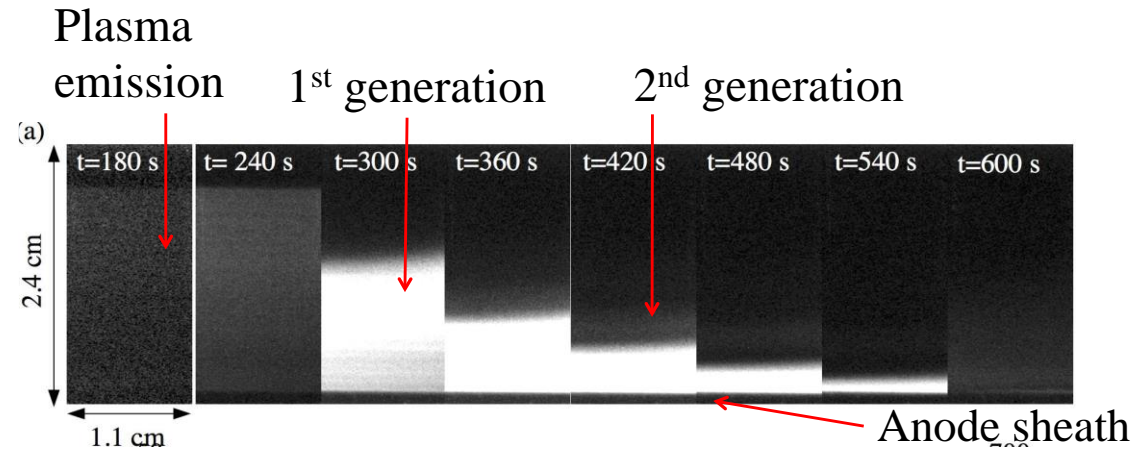
- Laser Induced Fluorescence (tunable laser diode)



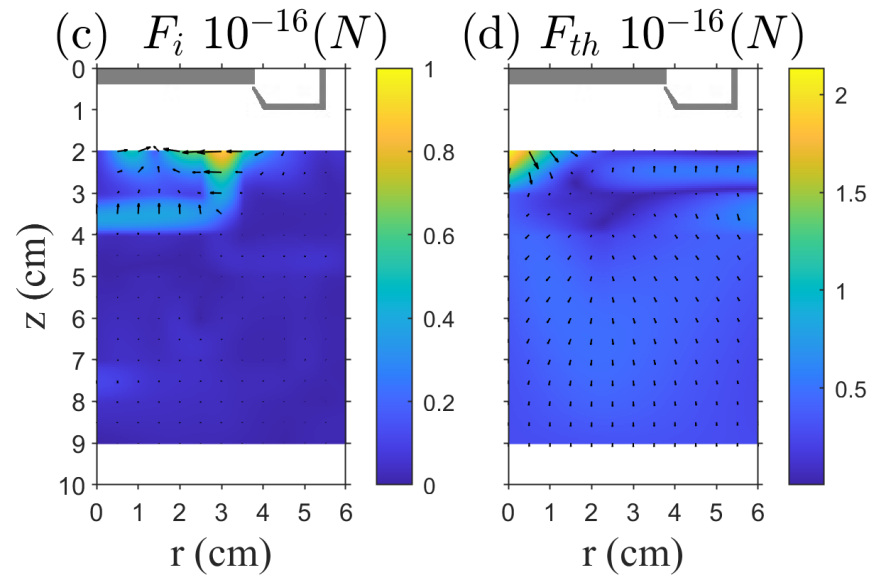
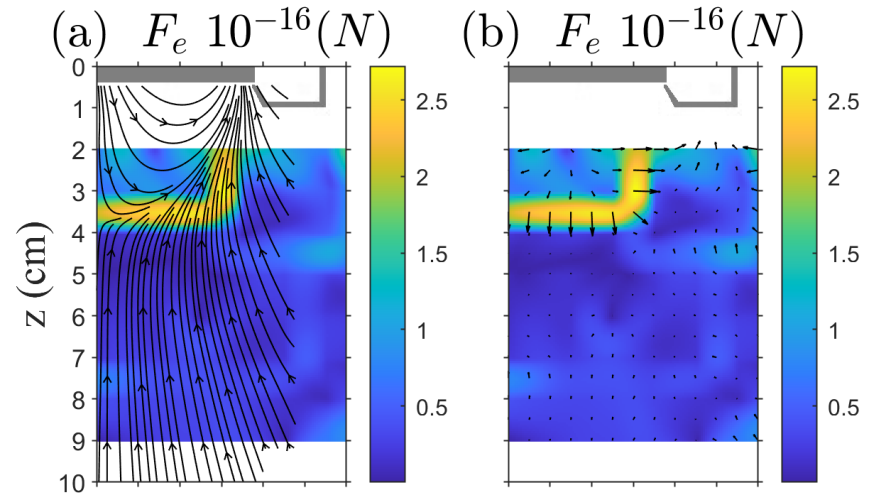
$\nu = c(\nu_l - \nu_0)/\nu_l$; ν_0 : transition frequency of an atom at rest, ν_l : the laser frequency

$$\text{Doppler shift: } k_b T = \frac{\lambda_0^2 M}{8 \ln 2} \Delta \nu^2$$

Laser scattering on the dust cloud during the transport of W nanoparticles towards the anode (classical DC discharges)



- $V \sim 0.004 \text{ cm/s} = 14.5 \text{ cm/h}$
- 2nd generation appears in the space freed by the 1st generation



- ❑ **Analogue of dust particles of ISM, planet satellites**

- ❑ **New materials, technologies:** superior properties to those of bulk materials
 - High surface area to volume ratio
 - Photo-emission wavelength decrease with the size decreases size
 - Lower melting temperature
 - Stronger materials

Applications:

- Optics: thinner displays, photophores, UV filters
- Electronics: nanodevice, single electron emission quantum dots
- Energy: hydrogen storage, improvement of solar cell efficiency
- Chemical: molecular sensor; catalyst
- Medicine: drug carriers, in-vitro imaging, cancer treatment